Critical Polyelectrolyte Adsorption Under Confinement: Planar Slit, Cylindrical Pore, and Spherical Cavity

A. G. Cherstvy[1,2,3]

[1] *Institute of Complex Systems, ICS-2, Forschungszentrum Jülich, 52425 Jülich, Germany*

[2] *Institute for Physics and Astronomy, University of Potsdam, 14476 Potsdam-Golm, Germany*

[3] *MPI for Physics of Complex Systems, Nöthnitzerstr. 38, 01187 Dresden, Germany*

Received 7 September 2011; revised 2 December 2011; accepted 21 December 2011
Published online 12 January 2012 in Wiley Online Library (wileyonlinelibrary.com). DOI 10.1002/bip.22023

ABSTRACT:

We explore the properties of adsorption of flexible polyelectrolyte chains in confined spaces between the oppositely charged surfaces in three basic geometries. A method of approximate uniformly valid solutions for the Green function equation for the eigenfunctions of polymer density distributions is developed to rationalize the critical adsorption conditions. The same approach was implemented in our recent study for the "inverse" problem of polyelectrolyte adsorption onto a planar surface, and on the outer surface of rod-like and spherical obstacles. For the three adsorption geometries investigated, the theory yields simple scaling relations for the minimal surface charge density that triggers the chain adsorption, as a function of the Debye screening length and surface curvature. The encapsulation of polyelectrolytes is governed by interplay of the electrostatic attraction energy toward the adsorbing surface and entropic repulsion of the chain squeezed into a thin slit or small cavities. Under the conditions of surface-mediated confinement, substantially larger polymer linear charge densities are required to adsorb a polyelectrolyte inside a charged spherical cavity, relative to a cylindrical pore and to a planar slit (at the same interfacial surface charge density). Possible biological implications are discussed briefly in the end. © *2012 Wiley Periodicals, Inc. Biopolymers 97: 311–317, 2012.*

Keywords: polymers; adsorption; electrostatics; confinement

This article was originally published online as an accepted preprint. The "Published Online" date corresponds to the preprint version. You can request a copy of the preprint by emailing the Biopolymers editorial office at biopolymers@wiley.com

INTRODUCTION

Adsorption of polyelectrolyte (PE) chains onto oppositely charged surfaces[1,2] has a number of important biological and technological applications. They range from DNA nanoscale wrapping in nucleosomes[3–5] and RNA/DNA assembly inside viral capsids[6,7] to PE coating of colloidal particles, applications in paper making and food industry. The subject of PE adsorption onto planar and curved surfaces for flexible[8–13] and semiflexible[14–17] chains has been studied thoroughly theoretically. The analytical results are supplemented by a wealth of data from computer simulations.[18–31]

One important question is about the condition for the critical adsorption of PE chains onto oppositely charged surfaces. It defines the minimal surface and PE linear charge densities above which the PE-surface electrostatic (ES) attraction overcomes the entropic losses for a polymer being adsorbed near the interface. The critical adsorption transition is thus defined as a coexistence between the PE bound and unbound states. The location of this adsorption–desorption threshold is a sensitive function of the surface charge

Correspondence to: A. G. Cherstvy; e-mail: a.cherstvy@gmail.com
Contract grant sponsor: Deutsche Forschungsgemeinschaft (DFG)
Contract grant number: CH 707/5-1

density σ, the PE linear charge density, the persistence length of the polymer l_p, the Debye screening length λ_D, and temperature T.

In confined spaces, the adsorption characteristics of flexible PEs naturally differ from those anticipated for the "inverse" problem of PE adsorption onto a planar surface as well as on the outside of cylindrical and spherical objects, see Ref. [35]. Energetically, the distribution of the ES potential between the two charged walls is altered qualitatively compared to a single-plane-potential when the plane-plane separations are $\leq\lambda_D$. Entropically, the number of conformational degrees of freedom of a polymer chain is altered drastically once the dimensions of the confining cavity shrink to several l_p. In the current article, we elucidate quantitatively this enthalpy–entropy trading in application to adsorption of flexible PE chains between the two (oppositely) charged planes and inside cylindrical and spherical attractive voids.

The PE adsorption onto curved surfaces poses a number of theoretical challenges, even on the level of Gaussian chains confined in the Debye–Hückel potential of an interface immersed in electrolyte solution. A number of approaches have been developed in the literature to unravel the critical conditions for adsorption of weakly charged PEs onto oppositely weakly charged curved surfaces. These include, e.g. the well-accepted variational method by Muthukumar et al.,[32] exact solutions in approximate potentials by Winkler et al.,[33,34] as well as the recent WKB (Wentzel–Kramers–Brillouin) technique developed by Cherstvy et al. in Ref. 35.

Theoretically, the confinement of neutral flexible and semiflexible chains in different geometries (planar slits,[36–39] cylindrical pores,[40–47] and spherical cavities[48,49]) have attracted the attention of researchers for decades. A number of trends for the polymer confinement are also available from computer simulations.[50–53] The problem of polyelectrolyte confinement by charged adsorbing walls is much less studied. The importance of this PE "caging" effect and some enhancement of ES attraction for PE adsorption in slits and cylindrical pores were mentioned already long ago.[54] Precise implications of these effects onto the critical PE adsorption have however not been investigated. We bridge this gap in the present study.

From the experimental perspective, the equilibrium adsorption isotherms of PEs onto charged surfaces in some cases exhibit a nonmonotonous dependence on the ionic strength. At low salinity, the ES stiffening of PE chains impedes their surface deposition, whereas at high salt levels the PE-surface ES attraction is progressively shielded and the adsorption degree is diminished as well, see Ref. 55. In that paper, it was shown (both experimentally and by computer simulations) that the properties of PE adsorption inside charged cavities are severely altered when the cavity size becomes comparable to the polymer radius of gyration.

Here, we want to mention a large set of experimental data from the P. Dubin lab on critical PE adsorption onto oppositely charged spherical and cylindrical micelles,[56,57] dendrimer molecules,[58] and some charged proteins,[59,60] monitored both for flexible and semiflexible PEs. The experimental data for critical PE deposition inside charged cavities are much sparser. This fact does not allow us to compare directly the theoretical trends presented below with the real experimental observations (in a manner we did in Ref. 17 for the critical PE-sphere adsorption and Dubin's data on PE complexation with spherical micelles).

This article is structured as follows. First, we describe the general principles of theoretical modeling of PE ES-driven adsorption onto oppositely charged interfaces. In particular, we focus on the WKB method for the Green function equation in the ground state dominance limit. The regimes of applicability of theoretical models and approximations employed are critically discussed. In the next section, the ES potentials are calculated for the three adsorption geometries, within the linear Poisson–Boltzmann (PB) theory. With these potentials at hand, the critical conditions for PE adsorption inside a planar slit, cylindrical pore, and a spherical cavity are computed. Finally, possible directions for further extensions of the model are overviewed.

MODELING PE ADSORPTION

Approximations

The PE chains are attracted toward an adsorbing interface immersed in electrolyte solution by screened Coulomb potential created in its vicinity. The interface bears a homogeneous surface charge density σ and is impenetrable to solvent molecules and PE chains. Cylindrical and spherical cavities have radius a, while the plane–plane separation is $2a$, see Figure 1. The solvent is treated as a continuum medium with the dielectric constant of $\varepsilon = 80$.

We implement the standard linear PB theory to compute the ES potential profiles near the charged surfaces. This Debye–Hückel theory provides a self-consistent description of ionic atmosphere of mobile point-like charges in electrolyte solutions. Ionic profiles obey the Boltzmann distributions and the electroneutrality of the surface with its mobile ions is automatically preserved in all three geometries. The ES potentials are calculated for a constant surface charge density (not at a constant-potential or within more elaborate models of charge-regulation[61]). With the well-known limitations of the linear PB model in mind (not

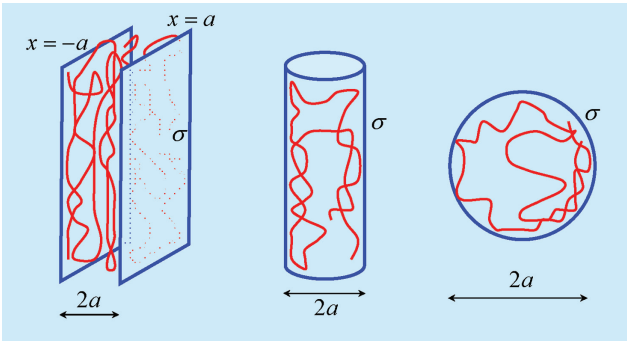

FIGURE 1 A pictorial representation of adsorption geometries considered.

valid for highly charged surfaces and multivalent cations, neglects saturation and close-packing effects for ions, etc.), these screened Coulomb potentials provide an analytically tractable description of ES-driven PE adsorption in the model.

Equilibrium ES potential profiles created in electrolyte near the charged surface are assumed to be insensitive to the adsorption of oppositely charged PE chains. Thus, a PE layer formed near the interface effectively leads to its overcharging, when the mobile ions from electrolyte and the PE charges are counted together. This drawback of the model can be resolved when the distributions of PE and electrolyte charges are found self-consistently, as in Refs. 62 and 63. The corresponding set of coupled differential equations is however only amenable to a numerical analysis. Hence, below we implement a simplistic but analytically tractable way to tackle the problem of PE adsorption. The adsorption–desorption threshold demarcates the parameter space into the regions of ES-bound PE-surface states and quasi-free polymers exploring their entropy in the bulk.

A weak-adsorption limit is investigated for weakly charged PEs, below the Manning counterion condensation threshold,[64,65] with no counterion-mediated attraction[66,67] between the PE segments. The linear PE charge density is $\rho = e_0/b_0$, where e_0 is the elementary charge and b_0 is the PE intercharge separation. The latter is set to be larger than the Bjerrum length, $b_0 > l_B = e_0^2/(\varepsilon k_B T)$. Both σ and ρ are assumed to be constant in the course of adsorption (no adsorption-mediated charge regulation, neither on the interface nor on the PE chain). The PEs are present at low concentrations in solution, so that the adsorption of a single polymer is examined, and not the entire PE-surface adsorption isotherm for a varying amount of PE in the bulk. Another limitation is that, for this mean-field theory to be applicable, the Debye screening length has to encompass many charges, both in electrolyte and on the PE chain.

The most severe limitation of the model is the Gaussian character of adsorbing PEs, without explicit salt dependence of the chain bending rigidity being taken into account. The latter can be incorporated in the final results via the well-known ES stiffening for flexible PEs.[32,68] An adsorbing PE is modeled as a long Gaussian polymer with the persistence length $l_p = b/2$. This length the shortest length-scale in the problem and strictly speaking the radius of surface curvature cannot be smaller than the Kuhn length b. The conditions of the critical PE adsorption into small cylindrical and spherical cavities can thus interfere with these model applicability regimes, so that the scaling relations obtained below in this limit are to be taken with caution. We neglect possible polymer knotting and entanglements[69] upon adsorption as well as excluded volume effects and steric constraints that might limit the amount of PE adsorbed, particularly for dense PE layers realized well above the adsorption transition.

Approach

A dimensionless universal adsorption parameter δ that we use below couples the strength of ES PE-surface attraction, temperature, chain persistence, and surface curvature. It can be written via the interaction parameter $\theta = 4\pi|\rho\sigma|/(\varepsilon k_B T\kappa)$ as

$$\delta = \frac{6a^3\kappa\theta}{b} = \frac{24\pi a^3|\rho\sigma|}{\varepsilon k_B T b}, \qquad (1)$$

where $\kappa = 1/\lambda_D$. The PE adsorption takes place when this adsorption parameter exceeds some critical value, $\delta > \delta_c$. This transition corresponds to the formation of a first bound PE state that emerges, e.g., when the surface charge density exceeds a critical value, $\sigma > \sigma_c$. Finding the dependence of σ_c on environmental conditions and model parameters such as κ, T, a, b is the main objective of this article. A swelling of PE layer and a desorption of PE chains can be triggered by higher temperatures, rise in the ionic strength, or a reduction of the surface/PE charge density, all favoring entropically dominated polymer state in solution.

The polymer chain is assumed to be sufficiently long (at least a dozen of Kuhn segments, $L \gg b$), that renders the ground state dominance approximation applicable. The equilibrium conformational properties of a polymer are described by the probability density function $G(\mathbf{r}, \mathbf{r}'; L)$, the Green function. Here $\mathbf{r}' = \mathbf{r}(0)$ and $\mathbf{r} = \mathbf{r}(L)$ are the positions of the polymer end points. For a PE chain in an attracting Debye–Hückel surface field $V_{DH}(\mathbf{r})$ the Green function obeys the equation

$$\left(\frac{\partial}{\partial L} - \frac{b}{6}\nabla_{\mathbf{r}}^2 + \frac{V_{DH}(\mathbf{r})}{k_B T}\right) G(\mathbf{r}, \mathbf{r}'; L) = \delta(\mathbf{r} - \mathbf{r}')\delta(L). \qquad (2)$$

The Laplacian $\nabla^2_{\mathbf{r}} G(\mathbf{r},\mathbf{r}';L)$ describes the conformational entropy of the polymer. For the bound PE-surface states the solution of this equation has to satisfy the boundary conditions of $G = 0$ at the adsorbing surface and far away from it. The PE-interface attraction (per unit polymer length) is written via the surface ES potential ψ as follows $V_{\mathrm{DH}} = -|\psi\rho|$. The standard procedure to find the solution of Eq. 2 is the eigenfunction expansion,

$$G(\mathbf{r},\mathbf{r}';L) = \sum_n \Psi_n^*(\mathbf{r}')\Psi_n(\mathbf{r})e^{\mu_n L}. \tag{3}$$

For long polymers, the lowest eigenvalue $\mu \equiv \mu_0$ gives the dominant contribution to the Green function ($\mu > 0$ for the bound states). The following equation is then valid for the eigenfunction of the ground state $\Psi \equiv \Psi_0$,

$$\left(-\frac{b}{6}\nabla^2_{\mathbf{r}} + \frac{V_{\mathrm{DH}}(\mathbf{r})}{k_{\mathrm{B}}T}\right)\Psi(\mathbf{r}) = -\mu\Psi(\mathbf{r}). \tag{4}$$

Below, the WKB technique is employed to solve this eigenvalue equation for the conditions of weak PE-surface adsorption. Recently, we applied the same method to rationalize the scaling characteristics for the "inverse" problem of PE adsorption onto a planar surface, and on the outside of cylindrical and spherical interfaces.[35] To save space here, we address the reader to Section III of Ref. 35 where a detailed description of the WKB method is provided.

DISTRIBUTION OF THE ES POTENTIAL

In this section, we calculate the Debye–Hückel potentials for a planar slit, cylindrical pore, and spherical cavity. Two different methods are implemented for the two possible choices of the potential variation. In the first case, we limit ourselves only to the regions of space in between the charged surfaces, ψ_{in}, assuming the potential to be constant outside. This provides a somewhat simpler (denoted by symbol *s*) solution for the potential. In the second situation, the potential is computed in the entire space, with the charge density σ forming a potential distribution both from the inner (in) surface and into the outer (out) electrolyte. The corresponding potentials are denoted as ψ_{in} and ψ_{out}.

The potentials are continuous on the charged interface obeying the Gauss theorem there. Both choices satisfy zero derivative of ψ at the mid-point of the slit, at the cylinder axis, and in the centre of the sphere. The correct values of the surface potential in the limit of well-separated planes and large rods/spheres ($a \to \infty$) are attained too. In the limit of $\kappa a \ll 1$, however, the second choice gives rise to finite potentials, while a simpler method results in diverging surface potential values. As shown in the next section, this difference in the asymptotic behavior of potentials affects dramatically the PE critical adsorption transition in the limit $\kappa a \ll 1$.

The ES potential inside a planar slit is $\psi_{\mathrm{s,in}}(x) = \psi_0 \frac{\cosh(\kappa x)}{\sinh(\kappa a)}$ for a simpler situation, while the field from an isolated plane decays exponentially, $\psi_{\mathrm{s,out}}(x) = \psi_0 e^{-\kappa x}$. Below, we use the notation $\psi_0 \equiv 4\pi\sigma/(\varepsilon\kappa)$ and $x > 0$. The second method with a continuous potential at the boundary gives

$$\psi_{\mathrm{in}}(x) = \psi_0 f_1(\kappa a)\cosh(\kappa x)$$

and

$$\psi_{\mathrm{out}}(x) = \psi_0 f_1(\kappa a)\cosh(\kappa a)e^{\kappa a}e^{-\kappa x},$$

with the definition

$$f_1(\kappa a) = \frac{2}{\sinh(\kappa a) + \cosh(\kappa a)}.$$

For a charged cylindrical pore $\psi_{\mathrm{s,in}}(r) = \psi_0 \frac{I_0(\kappa r)}{I_1(\kappa a)}$ and $\psi_{\mathrm{s,out}}(r) = \psi_0 \frac{K_0(\kappa r)}{K_1(\kappa a)}$, while we obtain

$$\psi_{\mathrm{in}}(r) = \psi_0 f_2(\kappa a) I_0(\kappa r)$$

and

$$\psi_{\mathrm{out}}(r) = \psi_0 f_2(\kappa a)\frac{I_0(\kappa a)}{K_0(\kappa a)}K_0(\kappa r).$$

Here, we denote

$$f_2(\kappa a) = \frac{2K_0(\kappa a)}{K_0(\kappa a)I_1(\kappa a) + K_1(\kappa a)I_0(\kappa a)},$$

the distance r from the cylinder axis is $a > r > 0$, and I_n and K_n are the modified Bessel functions of the second order.[70]

For a spherical cavity we have $\psi_{\mathrm{s,in}}(r) = \frac{\psi_0 \kappa a^2}{\kappa a\cosh(\kappa a) - \sinh(\kappa a)}\frac{\sinh(\kappa r)}{r}$ and $\psi_{\mathrm{s,out}}(r) = \psi_0 \kappa a^2 \frac{e^{\kappa a}}{1+\kappa a}\frac{e^{-\kappa r}}{r}$. For the second situation we get

$$\psi_{\mathrm{in}}(r) = \psi_0 \kappa a^2 f_3(\kappa a)\frac{\sinh(\kappa r)}{r}$$

and

$$\psi_{\mathrm{out}}(r) = \psi_0 \kappa a^2 f_3(\kappa a)\sinh(\kappa a)e^{\kappa a}\frac{e^{-\kappa r}}{r},$$

with the definition

$$f_3(\kappa a) = \frac{2}{\kappa a[\sinh(\kappa a) + \cosh(\kappa a)]}$$

and the radial coordinate $a > r > 0$.

Figure 2 shows these potential profiles. Note that at $\kappa a \ll 1$, the surface potentials $\psi_{\mathrm{s,in}}(a)$ from a simpler method for the closely separated planes, on a thin rod, and a small sphere diverge as $\propto 1/(\kappa a)$, $\propto 2/(\kappa a)$, and $\propto 3/(\kappa a)$, correspondingly. This divergence limits the applicability of the linear PB theory for ES potentials and modifies the critical adsorption condition in the limit of $\kappa a \ll 1$.

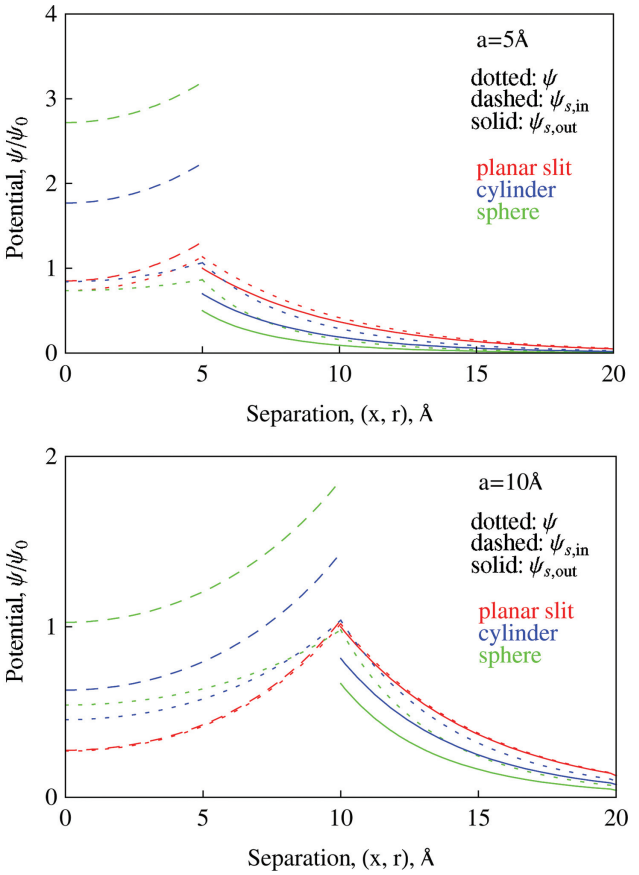

FIGURE 2 Distribution of the ES potential at λ_D=5 Å and for a = 5 and 10 Å. Red, blue, and green curves designate the slit, rod, and sphere quantities, respectively. The dotted curves illustrate ψ_{in} and ψ_{out} for the potential in the entire space, whereas simpler potential distributions $\psi_{s,in}$ and $\psi_{s,out}$ are shown as dashed and solid curves, correspondingly.

RESULTS FOR THE CRITICAL PE ADSORPTION

As described in details in Ref. 35, the polymer density near the interface scales with the square of the Airy Ai function that appears to be the eigenfunction of the WKB equation. The requirements of zero PE density on the adsorbing surface and far from it provide a condition for the argument of this function. The latter in turn defines the position of the adsorption–desorption equilibrium. This transition separates the energy-dominated bound and entropy-favored unbound states of the polymer in the attractive field of the interface.

In application to the problem of adsorption under confinement, the first bound state appears at a critical surface charge density σ_c at which the PE profile is zero on the surface and features a single peak in the mid-point between the planes (at $x = 0$) or at the cylinder axis or sphere centre (at $r = 0$). The $\delta_c(\kappa a)$ dependencies listed below are derived from this fundamental condition at $\mu = 0$. As the surface charge density σ grows, the two separate PE layers start forming at the two charged boundaries, with a deep in the polymer density at the mid-point. Upon further increase of σ, the PE layers shrink further and become more confined to the adsorbing interface. The quantitative analysis of the whole problem is quite cumbersome and in this letter we focus only on scaling regimes of the critical PE adsorption.

First, let us consider the case of more physical ψ_{in} ES potential distribution. We obtain that for a planar slit the critical adsorption parameter has the following functional form

$$\delta_c = \frac{6C^2\kappa a^3}{f_1(\kappa a)\left[\int_0^a dx\sqrt{\cosh(\kappa x)}\right]^2}, \tag{5}$$

with the asymptotic behavior of $\delta_c = 3C^2(\kappa a)^1$ at $\kappa a \ll 1$. Here, the constant C is given via the first zero ai of the Ai function as $C \equiv 2|ai_1|^{3/2}/\left(3\sqrt{6}\right) \approx 0.973$, according to the WKB derivation presented in Ref. 71. For a cylindrical pore, we get

$$\delta_c = \frac{6C^2(\kappa a)^3}{f_2(\kappa a)\left[\int_0^{\kappa a} du\sqrt{I_0(u)}\right]^2}, \tag{6}$$

with the scaling $\delta_c \approx 3C^2/(0.116 - \log(\kappa a))$ at $\kappa a \ll 1$. As κ increases, the critical adsorption strength grows too because of progressive screening of PE-surface ES attraction. Finally, for a spherical cavity the critical adsorption parameter $\delta_c = 24\pi a^3|\rho\sigma_c|/(\varepsilon k_B T b)$ obeys the relation

$$\delta_c = \frac{6C^2\kappa a}{f_3(\kappa a)\left[\int_0^{\kappa a} du\sqrt{\sinh(u)/u}\right]^2}, \tag{7}$$

with the $\delta_c = 3C^2$ scaling at $\kappa a \ll 1$. These $\delta_c(\kappa a)$ dependencies are the main result of this article, plotted as dotted

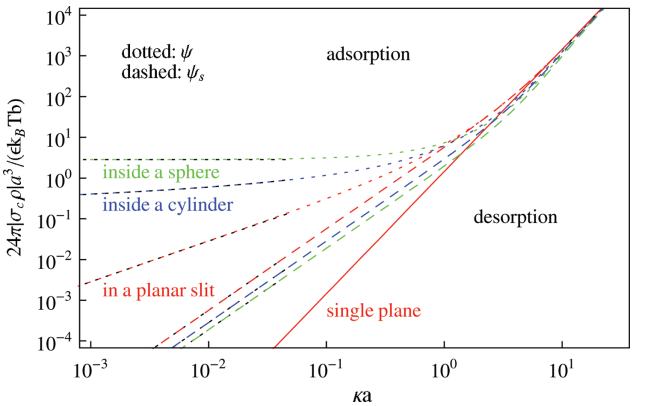

FIGURE 3 Critical adsorption parameter δ_c as a function of the degree of confinement and solution salinity. Scaling laws at $\kappa a \ll 1$ are shown as dotted black curves. Notations for the curves and color coding are the same as in Figure 2. Red solid line is the result for a planar interface.

curves in Figure 3. In the opposite limit of small curvature, at $\kappa a >> 1$, all three dependences naturally approach the WKB scaling for the PE critical adsorption onto an isolated planar surface, namely $\delta_c = 6C^2(\kappa a)^3/4$, see Ref. 35. Figure 3 illustrates that the transition to the planar limit takes place when the radius of surface curvature becomes comparable to the Debye screening length, i.e., at $\kappa a \sim 1$. Note that for the external PE adsorption, the crossover between the low- and high-curvature regimes of the critical PE adsorption $\delta_c(\kappa a)$ emerges at the same $\kappa a \sim 1$ value.

For a less physical (simpler) potential distribution from the attractive surfaces, $\psi_{s,in}$, all three geometries in $\kappa a \ll 1$ limit give rise to a quadratic dependence of δ_c with κa. Namely, in this limit for a planar slit we get $\delta_c = 6C^2(\kappa a)^2$, for a PE inside a cylindrical attractive tube $\delta_c = 3C^2(\kappa a)^2$, and for a PE encapsulated inside a sphere $\delta_c = 2C^2(\kappa a)^2$. Numeric results for $\delta_c(\kappa a)$ in the entire range of κa for the $\psi_{s,in}$ case are shown as dashed curved in Figure 3. Because of κa-dependent divergences of ES potentials in all three geometries at $\kappa a \ll 1$, we believe that these scalings are less physical than the ones obtained above for the ψ_{in} case, the dotted curves in Figure 3.

DISCUSSION AND CONCLUSIONS

In this article, we have investigated the implications of surface-induced confinement onto the properties of critical PE adsorption inside an oppositely charged planar slit, cylindrical pore, and spherical cavity. A consistent change in the scaling behavior in the limit of large curvature or low salt ($\kappa a \ll 1$) is predicted for ψ_{in} attractive ES potential. Namely, the entropic penalty of polymer confinement progressively increases as the chain of a definite length L is squeezed into a planar slit, a cylindrical pore, and finally into a spherical cavity. Therefore, progressively larger ES adsorption strengths are required to initiate the PE accumulation inside these adsorbing geometries. Note here that a partial polymer confinement in attractive cavities, considered in details in Ref. 54, was not allowed in the current model.

Analogously to the external PE adsorption discussed in Ref. 35, for the internal deposition the adsorbed PE chains have two degrees of freedom being confined in a planar slit, only one degree inside a cylindrical pore, and no freedom at all inside a spherical cavity. As a consequence, progressively increasing penalty for entropic confinement demands much larger surface charge densities to initiate the PE adsorption inside a spherical cavity, as compared to a cylindrical pore and planar slit. The dependencies for the universal adsorption parameter δ_c derived in Eqs. (5)–(7) can be associated with the critical values of physically relevant quantities. These are the critical slit thickness or void size ($a > a_c$), critical adsorption temperature ($T < T_c$), critical PE linear and surface charge densities ($\rho > \rho_c$, $\sigma > \sigma_c$), as well as a critical PE persistence length ($b < b_c$), all ensuring the onset on PE-surface complexation at $\delta > \delta_c$. Note also that the implications of the ES persistence length for flexible PEs, $l_p^{el} \propto \kappa^{-1}$, neglected in the current model, on the salt dependence of the adsorption–desorption transition can be rationalized according to the procedure proposed in Refs. 9 and 33.

The outcomes of this theoretical study can find their applications for PE adsorption onto topologically structured porous materials with some cavities for PE binding.[55] Another pertinent area is the encapsidation of single-stranded nucleic acid chains inside single-wall carbon nanotubes.[72–74] From the biological perspective, the adsorption of flexible single-stranded RNA genomes onto positively charged interiors of capsids of a number of viral families[75,77] can be a domain for applications of the current model (see for details the insightful investigation by Muthukumar et al.[6]).

To conclude, after this manuscript was submitted, we became aware of the variational approach of Ref. 76 for a finite-length PE chains inside a spherical oppositely charged cavity. A number of outcomes of this study are in line with our predictions. Specifically, the PE density profiles were shown to exhibit two modes of binding. At large adsorption strengths, a confined state of PEs near the inner spherical interface is realized, whereas at low PE-surface attraction a single polymer density peak at the mid-point/axis/centre is observed. Above the adsorption threshold, the width of the distribution becomes progressively smaller as the PE-surface ES attraction grows. It was argued that, due to confinement, both adsorbed and delocalized PE chains can correspond in the bound states of the system.

Important physical conclusion is that, in this trial-function theory, the interplay of PE-surface attraction and polymer entropic confinement gives rise to the existence of an optimal radius for encapsulation of a PE of a given length.[76] This radius was shown to be a nonmonotonic function of the universal adsorption parameter δ. At weak adsorption strength the optimal radius is large (entropy-dominated regime), at intermediate δ it reaches a minimum, while at strong adsorption (energy-dominated regime) the optimal capsid radius increases again. Using the $\delta \propto \sigma\rho/\kappa^3$ dependence introduced above, the authors could restore the behavior of the free energy minimum in the parameter space of the surface charge density, PE linear charge, and salinity of the solution (all appear nonmonotonous).

REFERENCES

1. Netz, R. R.; Andelman, D. Phys Rep 2003, 380, 1.
2. Dobrynin, A. V.; Rubinstein, M. Prog Polym Sci 2005, 30, 1049.

3. Luger, K.; et al. Nature 1997, 389, 251.
4. Richmond, T. J.; Davey, C. Nature 2003, 423, 145.
5. Cherstvy, A. G. J Phys Chem B 2009, 113, 4242.
6. Belyi, V. A.; Muthukumar, M. Proc Natl Acad Sci USA 2006, 103 17174.
7. Forrey, C.; Muthukumar, M. J Chem Phys 2009, 131, 105101.
8. Wiegel, F. W. J Phys A Math Gen 1977, 10, 299.
9. Muthukumar, M. J Chem Phys 1987, 86, 7230.
10. Baumgaertner, A.; Muthukumar, M. J Chem Phys 1991, 94, 4062.
11. Muthukumar, M. J Chem Phys 1995, 103, 4723.
12. Man, X.; Yan, D. Macromolecules 2010, 43, 2582.
13. Wang, Z.; et al. Macromolecules 2011, 44, 8607.
14. Netz, R. R.; Joanny, J. F. Macromolecules 1999, 32, 9026.
15. Kunze, K.-K.; Netz, R. R. Phys Rev Lett 2000, 85, 4389.
16. Schiessel, H. Macromolecules 2003, 36, 3424.
17. Cherstvy, A. G.; Winkler, R. G. J Chem Phys 2006, 125, 064904.
18. Chodanowski, P.; Stoll, S. J Chem Phys 2001, 115, 4951.
19. Kong, C. Y.; Muthukumar, M. J Chem Phys 1998, 109, 1522.
20. Welch, P.; Muthukumar, M. Macromolecules 2000, 33, 6159.
21. Messina, R.; Holm, C.; Kremer, K. J Polym Sci B 2004, 42, 3557.
22. Messina, R. J Chem Phys 2003, 119, 8133.
23. Ulrich, S.; et al. Macromolecules 2005, 38, 8939.
24. Stoll, S.; Chodanowski, P. Macromolecules 2002, 35, 9556.
25. Kaellrot, N.; Linse, P. J Phys Chem B 2010, 114, 3741.
26. Ulrich, S.; et al. Curr Opin Coll Interf Sci 2006, 11, 268.
27. Dobrynin, A. V. Curr Opin Coll Interf Sci 2008, 13, 376.
28. de Carvalho, S. J. EPL 2010, 92, 18001.
29. Larin, S. V.; et al. J Phys Chem B 2010, 114, 2910.
30. Cao, Q.; et al. Soft Matter 2011, 7, 506.
31. Carnal, F.; Stoll, S. J Phys Chem B 2011, 115, 12007.
32. van Goeler, F.; Muthukumar, M. J Chem Phys 1994, 100, 7796.
33. Winkler, R. G.; Cherstvy, A. G. Phys Rev Lett 2006, 96, 066103.
34. Winkler, R. G.; Cherstvy, A. G. J Phys Chem B 2007, 111, 8486.
35. Cherstvy, A. G.; Winkler, R. G. Phys Chem Chem Phys 2011, 13, 11686.
36. Freed, K. F. Adv Chem Phys 1972, 22, 1.
37. Chen, J. Z. Y.; Sullivan, D. E.; Yuan, X. EPL 2005, 72, 89.
38. Liu, Y.; Chakraborty, B. Phys Biol 2008, 5, 026004.
39. Milchev, A. J Phys Condens Matter 2011, 23, 103101.
40. Odijk, T. Macromolecules 1983, 16, 1340.
41. Burkhardt, T. W. J Phys A Math Gen 1995, 28, L629.
42. Park, P. J.; Chun, M.-S.; Kim, J.-J. Macromolecules 2000, 33, 8850.
43. Burkhardt, T. W. J Phys A Math Gen 1997, 30, L167.
44. Odijk, T. Phys Rev E 2008, 77, 060901(R).
45. Moebius, W.; Frey, E.; Gerland, U. Nano Lett 2008, 8, 4518.
46. Burkhardt, T. W.; Yang, Y.; Gompper, G. Phys Rev E 2007, 76, 011804.
47. Suo, T.; Yan, D. Polymer 2011, 52, 1686.
48. Sakaue, T.; Raphael, E. Macromolecules 2006, 39, 2621.
49. Morrison, G.; Thirumalai, D. Phys Rev E 2009, 79, 011924.
50. Cacciuto, A.; Luijten, E. Nano Lett 2006, 6, 901.
51. Cifra, P.; Benková, Z.; Bleha, T. J Phys Chem B 2008, 112, 1367.
52. Marenduzzo, D.; et al. Proc Natl Acad Sci USA 2009, 106, 22269.
53. Marenduzzo, D.; Micheletti, C.; Orlandini, E. J Phys Condenced Matter 2010, 22, 283102.
54. Lin, N. P.; Deen, W. M. Macromolecules 1990, 23, 2947.
55. Mishael, Y. G.; Dubin, P. L.; de Vries, R.; Kayitmazer, A. B. Langmuir 2007, 23 2510.
56. McQuigg, D. W.; et al. J Phys Chem 1992, 96, 1973.
57. Feng, X. H.; et al. Macromolecules 2001, 34, 6373.
58. Kayitmazer, A. B.; Shaw, D.; Dubin, P. L. Macromolecules 2005, 38, 5198.
59. Cooper, C. L.; et al. Biomacromolecules 2006, 7, 1025.
60. Kayitmazer, A. B.; et al. Biomacromolecules 2010, 11, 3325.
61. Ninham, B. W.; Parsegian, V. A. J Theor Biol 1971, 31, 405.
62. Podgornik, R. J Phys Chem 1992, 96, 884.
63. Borukhov, I.; Andelman, D.; Orland, H. J Phys Chem B 1999, 103, 5042.
64. Manning, G. S. Macromolecules 2001, 34, 4650.
65. Manning, G. S. J Phys Chem B 2007, 111, 8554.
66. Chi, P.; Li, B.; Shi, A. C. Phys Rev E 2011, 84, 021804.
67. Cherstvy, A. G. J Phys Chem B 2010, 114, 5241.
68. Dobrynin, A. V. Macromolecules 2005, 38, 9304.
69. Micheletti, C.; et al. Phys Rep 2011, 504, 1.
70. Gradshtein, I. S.; Ryzhik, I. M. Table of Integrals, Series, and Products; Academic Press: 1980.
71. Odijk, T. Macromolecules 1980, 13, 1542.
72. Gao, H.; et al. Nano Lett 2003, 3, 471.
73. Gao, H.; Kong, Y. Annu Rev Mater Res 2004, 34, 123.
74. Lulevich, V.; et al. Nano Lett 2011, 11, 1171.
75. Cherstvy, A. G. Phys Chem Chem Phys 2011, 13, 9942.
76. Wang, J.; Muthukumar, M. J Chem Phys 2011, 135, 194901.
77. Siber, A.; et al. Phys Chem Chem Phys 2012. DOI: 10.1039/C1CP22756D.

Reviewing Editor: Kenneth J. Breslauer